ATMOSPHERIC SCIENCE LETTERS
Atmos. Sci. Let. **17**: 208–215 (2016)
Published online 25 January 2016 in Wiley Online Library
(wileyonlinelibrary.com) **DOI:** 10.1002/asl.644

RMetS
Royal Meteorological Society

A geoengineering approach toward tackling tropical cyclones over the Bay of Bengal

S. Ghosh,[1,2]* A. Sharma,[1] S. Arora[1] and G. Desouza[1]

[1]*School of Mechanical and Building Sciences, Vellore Institute of Technology, Vellore, Tamilnadu, India*
[2]*School of Earth and Environment, University of Leeds, UK*

**Correspondence to:*
S. Ghosh, School of Mechanical and Building Sciences, Vellore Institute of Technology, Tamil Nadu, 632014, India.
E-mail: satgleeds@gmail.com

Received: 29 April 2015
Revised: 22 September 2015
Accepted: 24 November 2015

Abstract

The concept of seeding giant-sized ocean salt water aerosols in the eye-wall of a cyclonic storm abruptly increasing cloud condensation nuclei (CCN) concentration is investigated. To bring this to effect, design of a novel injection mechanism – a modified naval artillery shell, tailor made for the Indian Navy fleet, containing sea-salt solution to disperse the CCN is proposed. The effect of the seeding is modeled using a robust optimized warm rain microphysical scheme – amenable for quick local forecasts within the Weather Research and Forecast framework. The combined protocol results in a significant decrease in precipitation tendencies upon landfall.

Keywords: **cyclones; cloud seeding; aerosol injection; WRF; geoengineering**

1. Introduction

The eastern coast of India is routinely battered by severe tropical cyclones (e.g. Cyclonic storm Thane, Nilam, Viyaru, Phailin and more recently Hudhud). This article focuses on Cyclone Thane (25–31 December 2011) which wreaked havoc along south eastern coastal India. The coast is home to highly populous cities – many of them vulnerable, with a risk of flooding, affecting 13 million people.

Recent geoengineering methods used in the modification of cloud albedo by controlled emission of sea-salt spray into the atmosphere to offset global warming (Latham, 2002; Boyd, 2008; Lenton and Vaughan, 2009; Latham *et al.*, 2012a). Latham (1990) suggested an increase in the total droplet surface area of the cloud albedo by increasing the cloud droplet number concentration and reducing the droplet size by biasing the CCN to film mode sizes, a phenomenon known as marine cloud brightening (MCB). Latham *et al.* (2012b) explores the cooling effect of MCB over oceans as a method to mitigate cyclones. However, the most notable attempts at disrupting a cyclonic storm using geoengineering modifications are the STORMFURY experiments (Willoughby *et al.*, 1985), which relied on the seeding of a large amount of supercooled water in the cyclone using silver iodide. STORMFURY relied on directly targeting the eye-wall of the cyclone to deplete it of its energy. This method was subsequently disproved with the discovery that cyclonic storms possessed only a small amount of supercooled water which froze below 0 °C (Andreae *et al.*, 2004). Cotton *et al.* (2007) proposed the seeding of the peripheral rain bands of a cyclone with a large quantity of small-sized CCN to inhibit rain formation in these bands to inhibit cyclones. This method relies on intensification of the convection in the outer bands of the cyclone which in turn weakens the eye-wall by disrupting the convective forcing toward it. However, simulations of Typhoon Nuri (Krall and Cotton, 2012) show that the invasion of these small-sized CCN in the eye-wall has a synergistic effect on the cyclone intensification. There are other subsidiary articles that illustrate the concept of hygroscopic seeding of tropical cyclones (TCs) (Carrio and Cotton, 2010; Rosenfeld *et al.,* 2012; Hebener *et al.*, 2014). However, all these associated articles relate majorly to ice microphysics-mediated seeding hurricane Thane (as we discuss later) was predominantly governed by warm rain microphysics.

There is a rapid decrease in naturally produced sea-salt concentration above the mean sea level (MSL) (Blanchard *et al.*, 1984). Further, de Leeuw *et al.*, (2000) observed a logarithmic *decrease* in sea-salt concentrations with height. In this study, we explore the *effect of injecting artificially produced giant-sized sea-salt aerosol into the eye-wall of a cyclonic storm to enhance precipitation* prior to its landfall at a height of 200 m above MSL where contribution of sea-salt aerosols due to white capping is negligible. Like the previous attempts at cyclone modification, the central idea is the weakening of convection in the eye-wall of the cyclone. However, unlike STORMFURY, *this process seeks to induce greater precipitation using warm rain processes*. The cited tropical storms were mainly governed by warm rain microphysics. Enhancing warm rain within the eye-wall prevents ice-formation by averting the ascent of cloud droplets due to an early onset of precipitation. The only difference between a cloud seeding experiment and inducing precipitation in the eye-wall is with regard to the stronger up draughts and the rotational vorticity present in the latter. Therefore, shear generated turbulence inside the eye-wall

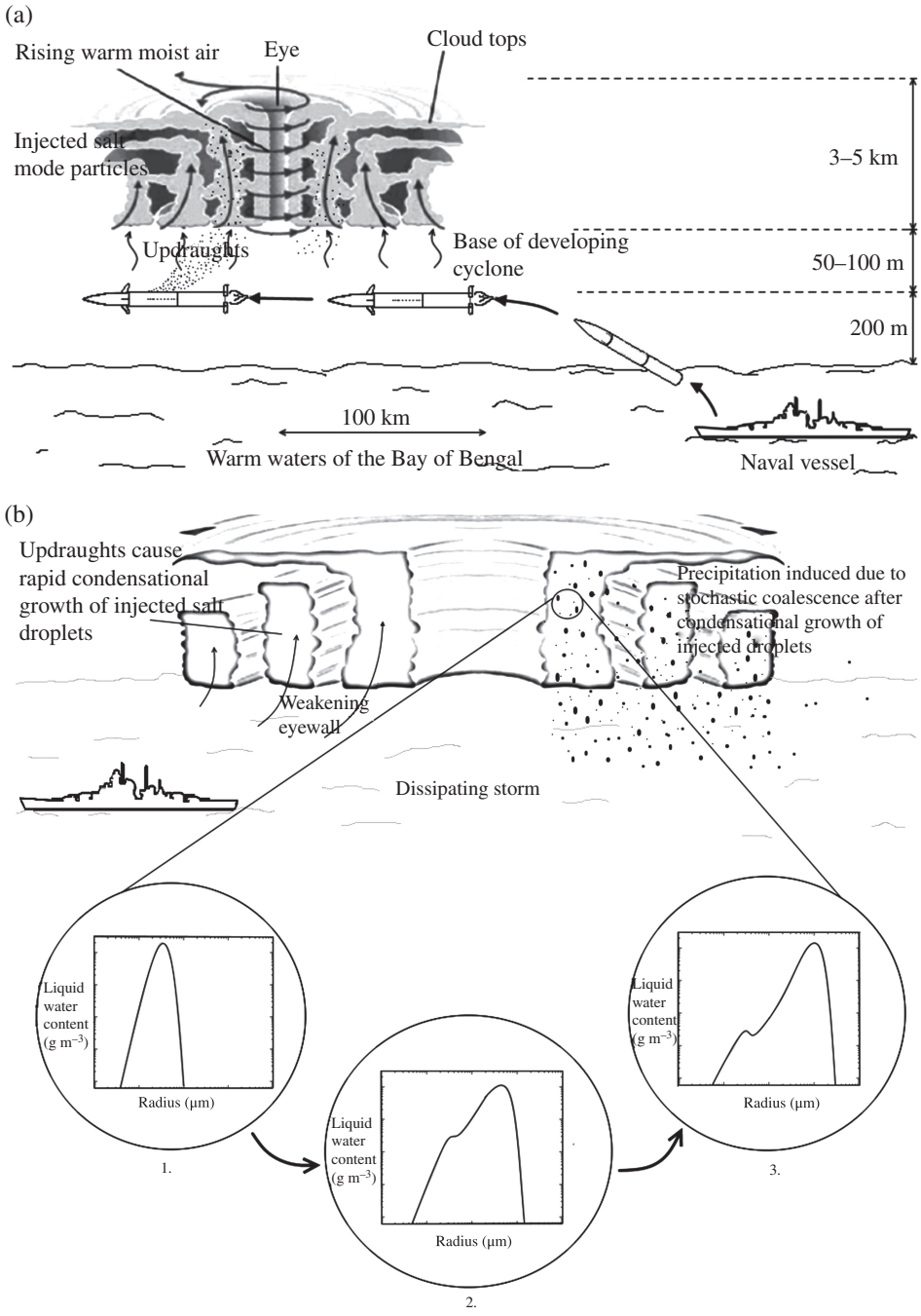

Figure 1. An outline of the proposed geoengineering mechanism scheme. (a) A light-weight artillery shell carrying the aerosol payload is launched from the vessel. Canards and fins are deployed: cruise altitude is reached as the propellant provides the necessary thrust. Sea-salt droplets in the jet mode are sprayed at the base of the developing cyclone which are then caught and carried along by the updraughts (figure not to scale) and (b) representative schematic of the time evolution of the droplet distribution leading to rain formation. 1) Initial single-humped distribution for liquid-water content. 2) Liquid-water distribution starts becoming double humped. 3) A fully developed bimodal spectrum causing rain ($g\,m^{-3}$).

would enhance the coalescence of all settling droplets (Ghosh *et al.,* 2005).

Another important difference between this study and the others is in the method of seeding. Traditional seeding experiments are aircraft dependent which restricts them to operate over safe areas. The use of unmanned, wind-driven Flettner-rotor vessels, which can be remotely steered beneath marine clouds to effect MCB, was proposed by Salter *et al.* (2008). For the present design, we propose a novel mechanism combining the flexibility afforded by aircrafts armed with autonomous capabilities.

The entire seeding process is summarized in Figure 1.

2. Microphysical characterization

A detailed microphysical chemical parcel model (henceforth called CPM) (O'Dowd *et al.*, 1999; Ghosh *et al.*, 2007) that employs the use of dynamical growth

equations to predict the growth of aerosol solution droplets by the condensation of water vapor in an updraught, on a size resolved droplet spectrum is used in this study.

Keeping in mind that a strong updraught is present in the range 2.5–10 ms^{-1} in a cyclone to ensure convective transport (Black *et al.,* 1994), the CPM is used to study the growth of natural and artificially injected sea-salt aerosols mimicking the conditions in the cyclonic rain bands. Even though Bay of Bengal (BOB) cyclones spend a majority of their lifespan over deep oceans, trace amounts of anthropogenic CCN such as sulfate aerosols are present in the local atmosphere of the cyclone (Jayaraman, 2001). These particles need to be added to the naturally present sea-salt aerosol spectrum (Figure 2(b)). When a cyclone approaches the coastline, aerosols get caught in the rising updraughts, initiating the process of condensational growth. The CPM incorporates the competing curvature (Kelvin effect) and solution effects on the equilibrium vapor pressure of the growing droplets based on the formation of a Kohler barrier, essentially the peak in the supersaturation versus radii curve (Seinfeld and Pandis, 1998). Our model results show that the Kohler barrier is exceeded for all the injected sea spray droplets with a median radius in the range of 15 μm. Eventually, these droplets attain the critical size of 20 microns required to initiate stochastic coalescence and cause rainfall (Ghosh *et al.*, 2005). The artificially injected spectrum is unique in the fact that the sizes and concentrations present work in tandem with the background spectrum to quickly achieve the requisite size for collision coalescence to set in.

The supersaturation curves (Figure 2(c)) obtained from the CPM reveal a clear cloud base 50 m above the point of injection.

2.1. Droplet trajectories and dispersion

The spray droplet trajectories were obtained using a commercial CFD code- Ansys Fluent– 15 on a $2 \times 2 \times 2$ m grid. A Discrete Phase Model (DPM) was used to simulate a secondary phase of discrete sea water droplets. Turbulence effects have been included by using the k-ε realizable turbulence model with default settings (ANSYS Fluent Theory Guide Release 12.1, 2009). The surface wave instability model is used, wherein the time of breakup and the resulting droplet size related to the fastest growing Kelvin–Helmholtz instability is accounted for (Reitz, 1987). The nozzle outlet is at the base of the domain. The trigger mass flow rate for spray ejection was set as 0.07 $kg\,s^{-1}$ after several numerical experiments with a cross-wind speed of 15 ms^{-1} (India Meteorological Department, 2012; Vinod *et al.*, 2014). The droplets continue to rise with increasing height – as is expected for the small droplets as the drag caused by the updraught considerably exceeds the gravitational force. These trajectories are validated using the by Ghosh and Hunt (1998) model for droplet behavior of spray jets in cross-winds.

The droplet size distribution of a plain orifice atomizer for a particular liquid is dependent on the flow rate (pressure at inlet) and the orifice diameter (Ayres *et al.*, 2001; ANSYS Fluent Theory Guide, 2009). For the purposes of this study, an orifice of constant diameter (1 mm) was analyzed at varying flow rates to obtain the optimum CCN size distribution. These results were validated by comparing the Sauter mean diameter (SMD) from a similarly sized nozzle. The numerically predicted SMD was 113 μm, only 9 μm greater than that analytically calculated (Merrington and Richardson, 1947; Omer and Ashgriz, 2011) as shown in Figure S1 (Supporting Information).This size distribution is essential for the successful alteration of the required cloud microphysics as there are only specific size combinations that result in enhanced autoconversion.

The near field dispersion generated from ANSYS Fluent were used to configure the far field Gaussian dispersion using a Diffusion code (Picardo and Ghosh, 2011) in moderate crosswinds causing a reduction in the CCN concentration of three orders of magnitude at a height of 50 m.

2.2. Growth by stochastic collision coalescence and onset of precipitation

The injected sea-salt droplets are biased toward the larger size, with the reduced surface to volume ratio of these droplets – the condensational growth rates are slower when compared with smaller droplets. The production of large aerosol particles by collision coalescence for the enhancement in precipitation is of crucial importance for the proposed mechanism to be successful.

The progression of droplet size distribution due to collision coalescence of drops is given by the stochastic collection equation. Figure 3 shows the time evolution of liquid-water mass as a function of total particle radius calculated using the Hall collection kernel based on the flux method (Bott, 1997).

3. The spraying mechanism

The efficacy of the proposed geoengineering technique crucially rests upon the efficiency of the ballistic hygroscopic seeding operation. The spraying mechanism proposed here is a ship borne Extended Range Guided Munition (ERGM) (Graham, 2004) modified to carry sea water as its payload. This shell has a caliber of 5 inches and can be fired from the main gun of the Indian Navy's Kolkata Class Guided Missile Destroyers. The spray is ejected out from a number of orifices drilled on to the surface of the shell. The cylindrical shell (length 135 cm and diameter 12.5 cm) is designed to hold 5–7 l of liquid to be ejected from 80–100 orifices of 1 mm diameter (Figure 2(a)). A piston assembly (actuated by a small explosive charge) pushes the fluid out through the orifices regulated by a sleeve valve. The opening and closing of the valves is regulated by servo motors

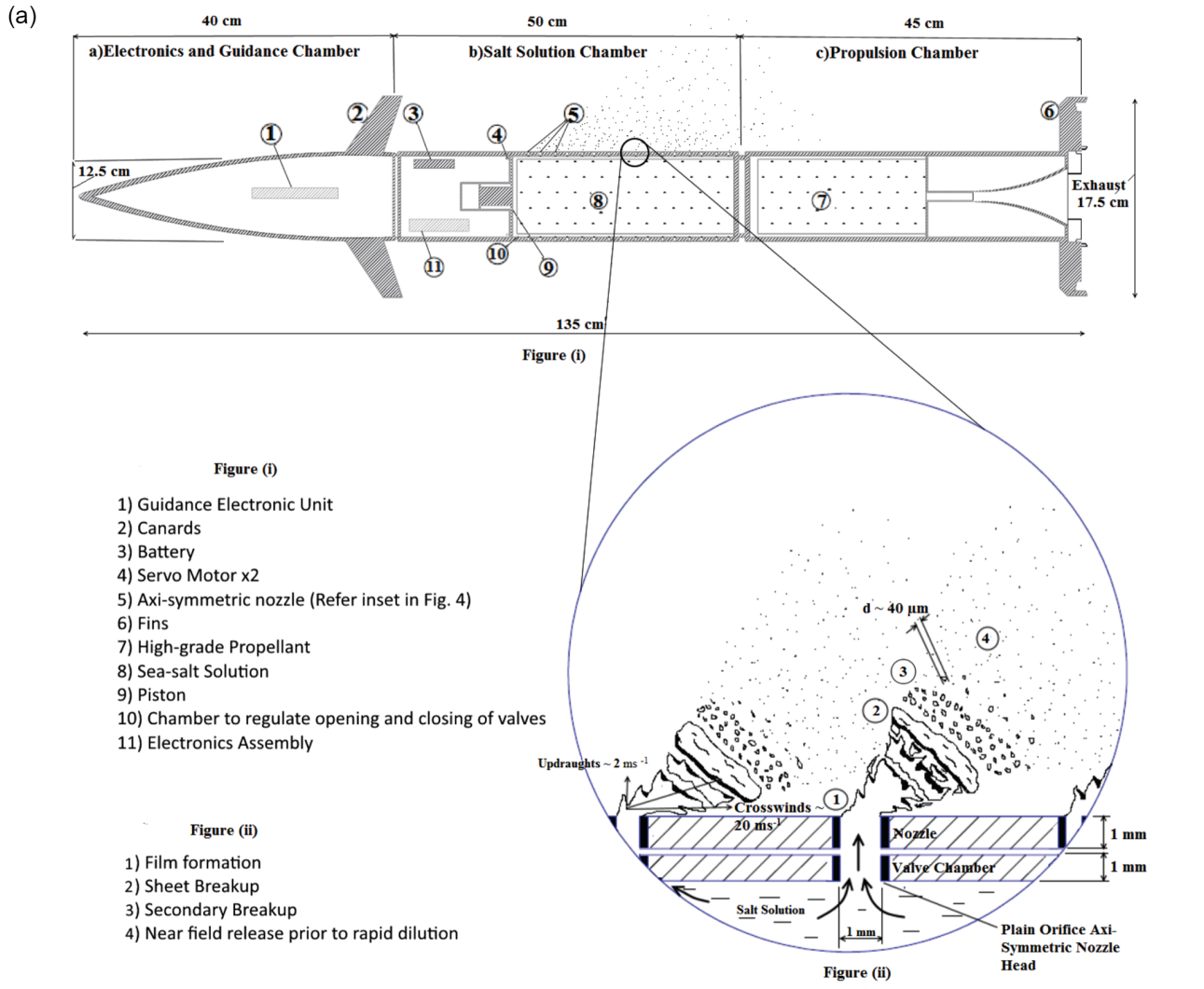

Figure 2. (a) Spray ejection and droplet breakup through an artillery shell (i) longitudinal cross-section (ii) Magnified view of the orifice and droplet breakup. (b) Aerosol spectra over the Bay of Bengal. The first curve shows the natural sulphate spectrum and the second, the film and jet modes of the natural sea-salt spectrum (Jayaraman, 2001; Ghanti and Ghosh, 2010). The curve on the right shows the artificially injected spectra. The positioning of the injected spectra is crucial – if it were positioned on the left, the droplets would have competed with the natural spectra for moisture and eventually reduced in size. However, if it were positioned on the right, they would have quickly gathered the smaller droplets and fallen due to inertia without making a significant contribution to the rainfall rate. Panel (c) shows the supersaturation profile for the natural and injected spectra, as obtained from the chemical parcel model (O'Dowd *et al.*, 1999). Note the rise in the height of the cloud base to 50 m for injected spectrum. This buffer height allows the injected droplets to activate and undergo condensational growth as they rise in the updraught.

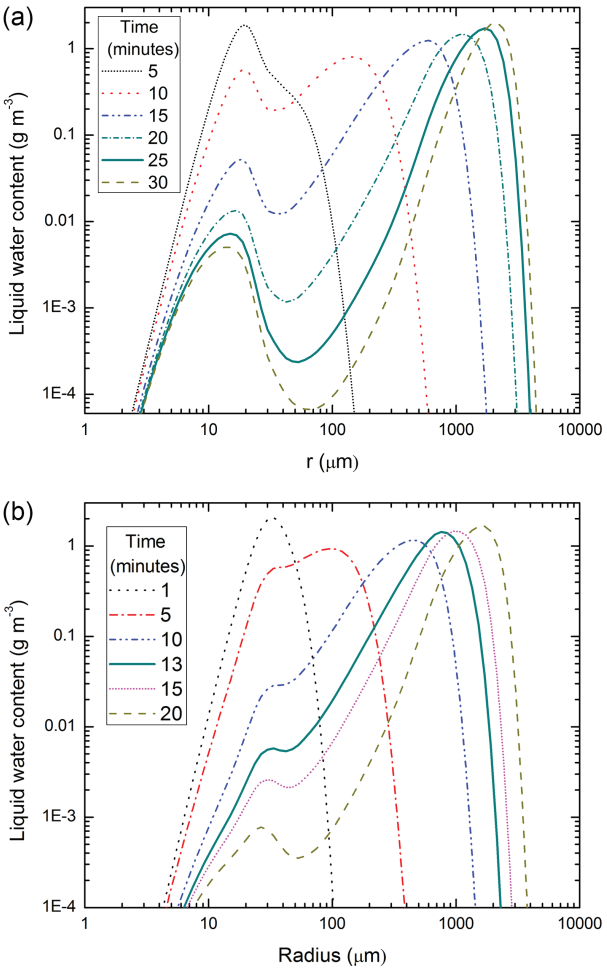

Figure 3. Time evolution of liquid-water mass. Panel (a) shows the unmodified spectra consisting only the naturally occurring sea-salt and sulphate aerosols (modal radius 18 μm). The time required to obtain a droplet radius of 1 mm is 25 min. Panel (b)shows modified spectra consisting of the injected and naturally occurring aerosols(modal radius 40 μm) for a total water content of 1.5 g m^{-3}. Note that the time to obtain a droplet radius of 1 mm through collision coalescence is reduced to 13 min for the modified spectrum after hygroscopic seeding, thus initiating hastened precipitation. The onset time of precipitation shows good agreement with analytical relations given by Ghosh and Jonas (1998).

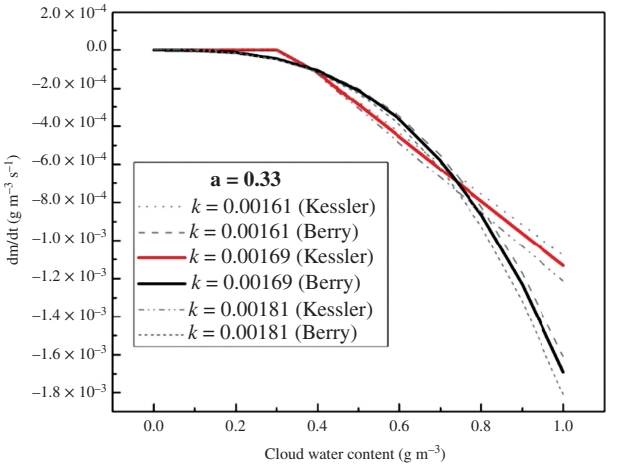

Figure 4. Overlapped mass-flux versus total cloud water content for Kessler schemes using Ghosh and Jonas (1998) (and references therein) – optimization of curves to include aerosol signatures into cyclone Thane microphysics. The bold lines show the closest correlation and have been used for the WRF simulations. The autoconversion rates and the threshold are represented by 'k' and 'a', respectively.

situated at the extremities of the payload bay. Streams of uncharged salt water are sprayed through a series of plain orifice atomizers of 1 mm diameter and 2 mm length retrofitted in the orifices across the surface of the artillery shell. With the proposed design, it is estimated that the seeding of an annular ring of thickness 50 m around the eye of a cyclone (15 km in diameter) will require 38601 of sea water. This equates to firing 640 shells (each shell can carry 6 lof payload). A deck gun of a conventional frigate has a fire rate of around 25 rounds per minute (Polmar, 2005). Thus, a constellation of 3–5 ships will theoretically complete the seeding operations in 5–10 min. The Indian Navy has about 24 frigates and destroyers in service as of today.

The shell will be guided to the precise location of the injection using a Guidance Electronic Unit (GEU), mounted in the nose cone of the projectile. Control surfaces in the form of canards will allow the GEU to maneuver the shell. Sensors used to measure the altitude, velocity and temperature of the atmosphere around the shell will also be present in the nose cone. At the pre-fed coordinates, the sleeve valve will open and the piston charge will deploy, releasing the salt water droplets.

It may be noted here that we assume that the described system will function as simulated in this study.

4. Optimization of autoconversion parameters and WRF simulations

The Kessler warm rain microphysics scheme (Kessler, 1969) used by the WRF-3.4.1 does not explicitly take into account the droplet size distribution and their number concentrations while predicting rainfall. It is important to rectify this, where the rainfall rates have been synthetically modified. A combination of the Kessler and Berry schemes (Ghosh and Jonas, 1998; Fournier *et al.*, 2005; Yin *et al.*, 2015) is used calculate optimized values of autoconversion rate and threshold by taking into account the combined effects of number and size of the droplets present in the cloud base. The value of the autoconversion rate (k1) was calculated to be 1.7×10^{-4} s^{-1} which represents a 70% increase from the default value. An autoconversion threshold of 0.3 g kg^{-1} (as opposed to a default value of 1 g kg^{-1}) yielded the greatest agreement between the linear Kessler and cubic Berry schemes (Figure 4).

Based on the reflectivity data for cyclone Thane, the cloud base around the eye-wall was placed at about 200 m above the sea (India Meteorological Department, 2012) where the temperatures are non-freezing. NASA's TRMM satellites revealed that on the 27th and 29th December 2011 majority of

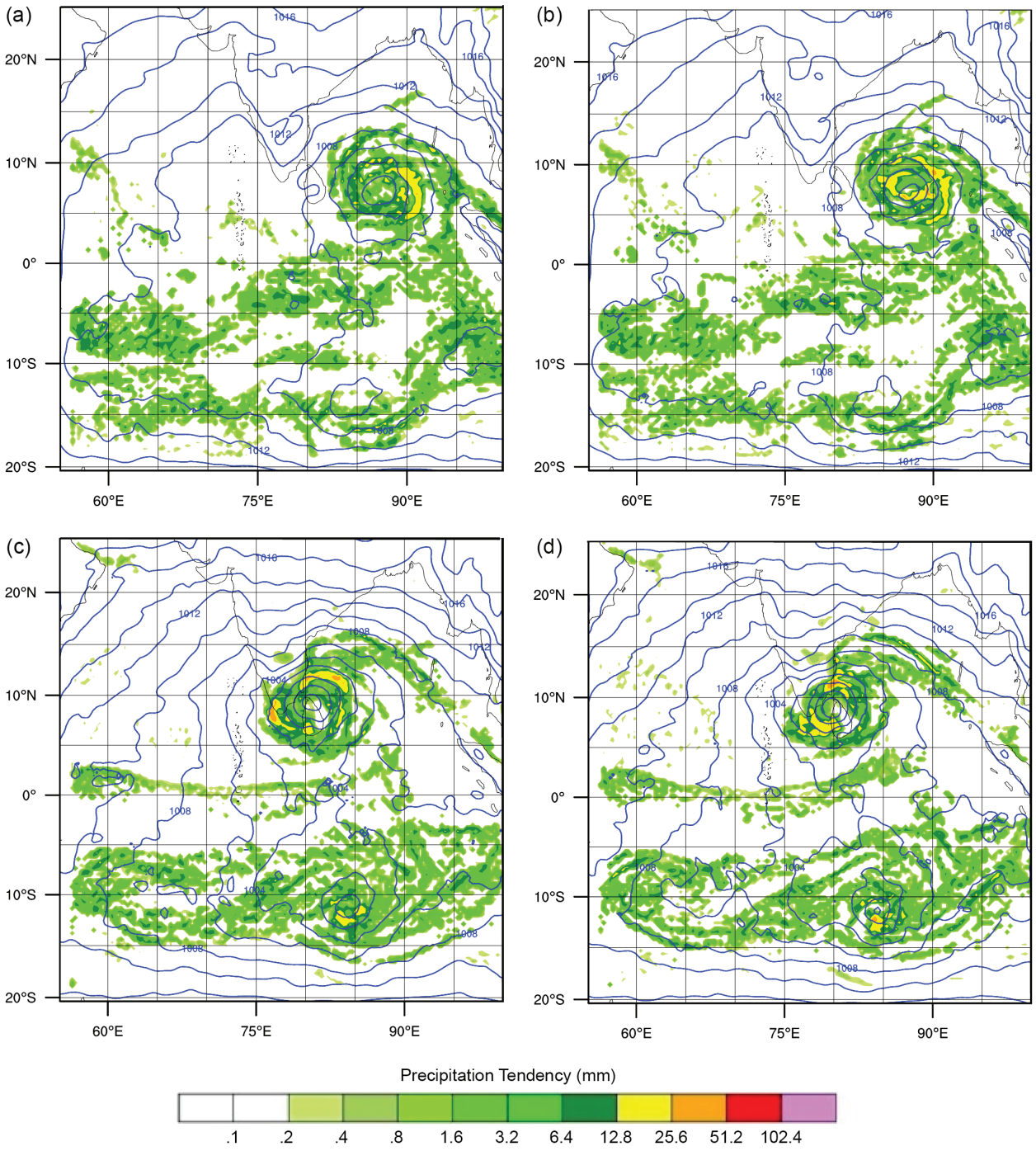

Figure 5. Precipitation tendencies (change of the intensity of precipitation during the last time period) for cyclone Thane over 6 h for (a) Run 1(Unseeded/control run): 25 December 2011 – 1500 UTC to 1800 UTC. (b) Run 2 (Seeded run): 2 December 2011 – 1500 UTC to 1800 UTC. (c) Run 1: 28 December 2011 – 2100 UTC to 29 December 2011 0000 UTC. (d) Run 2: 28 December 2011 2100 UTC – 29 December 2011 0000 UTC. Panel (b) shows an abrupt increase in precipitation in the final three hours of seeding. Just prior to landfall, a 50% decrease in precipitation tendency can be seen in the seeded run (d). As is expected, a marked increase in the rainfall rate is observed near the eye-wall of the cyclone seen as the bright yellow streak bordering the eye (a). The rainfall rate in Run-2 abates rapidly after the end of the seeding process and continues to reduce beyond the rates seen in Run 1 until the cyclone makes landfall. As can be seen in (d) the maximum precipitation tendency is restricted to 25 mm over the majority of the south eastern coast of India whereas in Run 1 (c) large swathes of land experience a precipitation tendency of 50 mm (marked orange). The spatial extent of the rain-bands is also visibly diminished as is seen when comparing (c) and (d).

the storm bands resided between 0 and 7 km above the mean sea level. The notion of using warm rain microphysics to simulate a cyclone was tested in a recent study by Wang (2001), who concluded that even though this led to early intensification of the cyclone, the final intensity was comparable with those produced by more complex models. Our own Thane simulations attests to this conclusion-runs with and without ice microphysics show only around 10% difference. The unification of the Kessler and Berry schemes by

Ghosh and Jonas (1998), along with the high degree of customizability offered by the WRF code allowed the modification of the autoconversion parameters. The nesting option provided within the WRF was used to pinpoint the seeded area, i.e. the eye-wall within the larger domain. Two-way feedback between the nested and the parent domains illustrated the effect of seeding the eye-wall exclusively. Validation runs using WRF Double Moment −5 microphysics with and without seeding were carried out (as shown in Figure S2), which show a similar trend as the warm rain runs, lending support to our view that computationally low-cost warm rain microphysics can indeed provide a fair estimate of cyclone progression and weakening.

The seeding is simulated for a period of 12 h, from 0600 UTC to 1800 UTC on the 25th of December in the test case (Cyclone Thane). The time step for the simulation was fixed at 180 s. The grid size used was 10 m for the larger domain and 2 m for the nested domain which corresponds to 19 and 4 km, respectively. The time step and geographical grid was scaled down for the nested domain by a factor of 7. Figure 5 compares the precipitation tendencies for the cyclone just after completion of the seeding.

5. Conclusions

In a seminal article on the geoengineering modification of marine cloud brightening, Latham *et al.* (2012a), showed how sea sprays can offset global warming. While in this process, precipitation was suppressed by the application of sea water, in the current research, precipitation in the cyclone is enhanced over preferred locations resulting in reduction of rainfall along the southeastern coast of India by up to 50%.

A carefully crafted design study is presented which accounts for the accurate delivery of sea-salt droplets into the eye-wall of a developing cyclonic storm. For the first time, the full spraying mechanism is articulated for a real-time ballistic discharge. Once the droplets permeate the cloud base, they are allowed to ascend to the cyclones womb through turbulent updraughts. This ascension and the subsequent activation process are rigorously modeled with the CPM yielding copious precipitation over the Bay of Bengal. Another important caveat explored is tied to the whole process of rapid dissemination of cyclone alerting mechanism (Ghosh *et al.*, 2014) using a well-tuned WRF run. This article marks out the conditions required for such an optimized WRF run as a function of the liquid discharge rate of the sprayed sea salt. Through a combination of these procedures, the article shows that Cyclone Thane when impregnated with the shown spectrum of sea water aerosols released 50 m below the eye-wall, when it is 900 km from the Indian coast, causes it to copiously precipitate over 24 h after injection. This causes a rapid depletion of precipitation tendencies at landfall. Finally, we wish to also add that observational studies with in-situ measurements of Hurricane Thane were very limited and future studies in this direction must focus on observational analyses as well.

Acknowledgements

The authors are grateful to Archit Verma for his help.

Supporting information

The following supporting information is available:

Figure S1. Correlation between numerically and analytically calculated Sauter mean diameters for varying flow rates.

Figure S2. Precipitation for the 25th of December for a full microphysics WDM 5 run including ice processes (left panel-a) contrasted with a Kessler only warm rain microphysics run (right panel-b). Note that almost identical precipitation tendencies are observed – the distribution of rain are very similar across peninsular India and the Indian Ocean for the two runs indicating that Cyclone Thane was operated upon by mainly warm rain microphysical processes.

References

Andreae MO, Rosenfeld D, Artaxo P, Costa AA, Frank GP, Longo KM, Silva-Dias MAF. 2004. Smoking Rain Clouds over the Amazon. *Science* **303**(5662): 1337–1342.

ANSYS® Academic Research. 2009. *Release 12.1, Help System, Fluent Theory Guide*. ANSYS Inc.

Ayres D, Caldas M, Semiaão V, Da GracëaCarvalho M. 2001. Prediction of the droplet size and velocity joint distribution for sprays. *Fuel* **80**(2001): 383–394.

Black RA, Bluestein HB, Black ML. 1994. Unusually strong vertical motions in a Caribbean Hurricane. *Monthly Weather Review* **122**: 2722–2739.

Blanchard DC, Cipriano RJ, Woodcock AH. 1984. The vertical distribution of the concentration of sea salt in the marine atmosphere near Hawaii. *Tellus Series B Chemical and Physical Meteorology B* **36**: 118–125.

Bott A. 1997. A flux method for the numerical solution of the stochastic collection equation. *Journal of the Atmospheric Sciences* **57**(2): 284–294.

Boyd PW. 2008. Ranking geoengineering scheme. *Nature Geosciencei* **1**: 722–724.

Carrio GG, Cotton WR. 2010. Investigations of aerosol impacts on hurricanes: virtual seeding flights. *Atmospheric Chemistry and Physics* **11**: 2557–2567.

Cotton , Zhang H, McFarquhar GM, Saleeby SM. 2007. Should we consider polluting hurricanes to reduce their intensity? *Journal of Weather Modification* **39**: 70–73.

Fournier N, Weston KJ, Dore AJ, Sutton MA. 2005. Modeling of wet deposition of reduced nitrogen over the British Isles using a Lagrangian multi-layer atmospheric transport model. *Quarterly Journal of the Royal Meteorological Society* **131**: 703–722.

Ghanti R, Ghosh S. 2010. The Great Indian haze revisited: Aerosol distribution effects on microphysical and optical properties of warm clouds over peninsular India. *Advances in Geosciences* **25**: 51–54.

Ghosh S, Hunt JCR. 1998. Spray jets in a cross-flow. *Journal of Fluid Mechanics* **365**: 109–136.

Ghosh S, Jonas PR. 1998. On the application of the classic Kessler and Berry schemes in Large Eddy Simulation models with a particular emphasis on cloud autoconversion, the onset time of precipitation and droplet evaporation. *Annales Geophysicae* **16**: 628–637.

Ghosh S, Davila J, Hunt JCR, Srdic A, Fernando HJS, Jonas PR. 2005. How turbulence enhances coalescence of settling particles with applications to rain in clouds. *Proceedings of the Royal Society A: Mathematical Physical and Engineering Science* **461**(2062): 3059–3088.

Ghosh S, Smith MH, Rap A. 2007. Integrating biomass, sulphate and sea-salt aerosol responses into a microphysical chemical parcel model: implications for climate studies. *Philosophical Transactions of the Royal Society A* **365**: 2659–2674, doi: 10.1098/rsta.2007.2082.

Ghosh S, Vidyasagaran V, Sandeep S. 2014. Smart cyclone alerts over the Indian subcontinent. *Atmospheric Science Letters* **15**(2): 157–158.

Graham J. 2004. Extended Range Guided Munition (ERGM) Program" ,NDIA International Armaments Technology Symposium and Exhibition.

Herbener SR, van den Heever SC, Carrió GG, Saleeby SM, Cotton WR. 2014. Aerosol indirect effects on idealized tropical cyclone dynamics. *Journal of the Atmospheric Sciences* **71**: 2040–2055.

India Meteorological Department, 2012 - Very Severe Cyclonic Storm THANE over the Bay of Bengal (25–31 December, 2011); A Report.

Jayaraman A. 2001. Aerosol radiation cloud interactions over the Indian Ocean prior to the onset of the summer monsoon. *Current Science* **81**(11): 1437–1445.

Kessler E. 1969. On the distribution and continuity of water substance in atmospheric circulation. *Meteorological Monographs* **32**: Amer. Meteor. Soc.: 84.

Krall G, Cotton WR. 2012. Potential indirect effects of aerosol on tropical cyclone intensity: Convective fluxes and cold-pool. *Atmospheric Chemistry and Physics Discussions* **12**: 351–385.

Latham J. 1990. Control of global warming? *Nature* **347**: 339–340.

Latham J. 2002. Amelioration of global warming by controlled enhancement of the albedo and longevity of low-level maritime clouds. *Atmospheric Science Letters* **3**: 53–58.

Latham J, Bower K, Choularthon T, Coe H, Connolly P, Cooper G, Caft T, Foster J, Gadian A, Galbraith L, Iacovides H, Johnston D, Launder B, Leslie B, Meyer J, Neukemans A, Ormond B, Parkes B, Rasch P, Rush J, Salter S, Stevenson T, Wang H, Wang Q, Wood R. 2012a. Marine cloud brightening. *Philosophical Transactions of the Royal Society A* **370**: 4217–4262.

Latham J, Parkes B, Gadian A, Salter S. 2012b. Weakening of hurricanes via marine cloud brightening (MCB). *Atmospheric Science Letters* **13**(4): 231–237.

de Leeuw G, Neele FP, Hill M, Smith MH, Vignati E. 2000. Sea spray aerosol production by waves breaking in the surf zone. *Journal of Geophysical Research* **105**(29): 397–29, 409.

Lenton TM, Vaughan NE. 2009. The radiative forcing potential of different climate geoengineering options. *Atmospheric Chemistry and Physics* **9**: 5539–5561.

Merrington AC, Richardson EG. 1947. The break-up of liquid sheets. *Proceedings of the Physical Society of London* **59**(33): 1–13.

O'Dowd C, Lowe JA, Smith MH. 1999. Observations and modeling of aerosol growth in marine stratocumulus – case study. *Atmospheric Environment* **33**: 3053–3062.

Omer K, Ashgriz N. 2011. Chapter. 24: Spray nozzles. In *Handbook of Atomization and Sprays*. Springer: Boston, MA.

Picardo JR, Ghosh S. 2011. Removal mechanisms in a tropical boundary layer: quantification of air pollutant removal rates around a heavily afforested power plant. In *Air Pollution-New Developments*, Moldoveanu A (ed). InTech Publishers: Croatia, doi: 10.5772/18348.

Polmar N. 2005. *The Naval Institute Guide to the Ships and Aircraft of the U.S. Fleet*, 18 ed. Naval Institute Press: Annapolis, MD.

Reitz RD. 1987. Modeling atomization processes in high-pressure vaporizing sprays. *Atomization and Spray Technology* **3**: 309–337.

Rosenfeld D, Woodley WL, Khain A, Cotton WR, Carrió G, Ginis I, Golden JH. 2012. Aerosol effects on microstructure and intensity of tropical cyclone. *American Meteorological Society* **93**: 987–1001.

Salter S, Sortino G, Latham J. 2008. Sea-going hardware for the cloud albedo method of reversing global warming. *Philosophical Transactions of the Royal Society* **A366**: 3989–4006.

Seinfeld JH, Pandis SN. 1998. *Atmospheric Chemistry and Physics: From Air Pollution to Climate Change. Cloud Physics*. John Wiley & Sons, Inc.; 777–840.

Vinod KK, Soumya M, Tkalich P, Vethamony P. 2014. Ocean–atmosphere interaction during Thane cyclone: a numerical study using WRF. *Indian Journal of Marine Sciences* **43**(7): 1–5.

Wang Y. 2001. An explicit simulation of tropical cyclones with a triply nested movable mesh primitive equation model: TCM3 part II: model refinements and sensitivity to cloud microphysics parameterization. *Monthly Weather Review* **129**: 1370–1394.

Willoughby HE, Jorgensen DP, Black RA, Rosenthal SL. 1985. Project STORMFURY: a scientific chronicle. *Bulletin of the American Meteorological Society* **66**(5): 1962–1983.

Yin J, Wang D, Zhai G. 2015. An attempt to improve Kessler-type parameterization of warm cloud microphysical conversion process using CloudSat observations. *Journal of Meteorological Research (Elsevier)* **29**: 82–92.